

Analysis of Scatterometer Observations of Saharan Ergs Using A Simple Rough Facet Model

Haroon Stephen and David G. Long

Brigham Young University Microwave Earth Remote Sensing Laboratory
459 Clyde Building, Provo, UT 84602, Email: hs92@et.byu.edu and long@ee.byu.edu

Abstract—The Sahara desert includes large expanses of sand dunes called ergs. These dunes are formed and constantly reshaped by prevailing winds. Previous study shows that Saharan ergs exhibit significant radar backscatter (σ°) modulation with azimuth angle (ϕ). We use σ° measurements observed at various incidence angles (θ) and ϕ from the NASA scatterometer (NSCAT), the Seawinds scatterometer aboard QuikSCAT (QSCAT), the ERS scatterometer (ESCAT) and the Tropical Rain Monitoring Mission's Precipitation Radar (TRMM-PR) to model the σ° response from sand dunes.

Sand dunes are modeled as a composite of tilted rough facets and small ripples. The dune fields are modeled as composed of many simple dunes. The σ° measured by the scatterometer from (θ , ϕ) look direction is the sum of the returns from all the rough facets in the footprint.

The model is applied to linear and transverse dunes with rough facets and Gaussian tilt distributions. The model results in a σ° response similar to the NSCAT and ESCAT observations over areas of known dune types in the Sahara. This analysis gives a unique insight into scattering by large scale sand bedforms.

I. INTRODUCTION

Deserts consist of diverse terrains primarily classified as rocky mountains, small- and large-scale-gravel zones and vast sand-seas called *hamadas*, *regs* and *ergs*, respectively. The ergs of the Sahara consist of large sand-dune fields which are variable due to the wind action [1].

Scatterometers measure radar backscatter (σ°) of the surface at various incidence (θ) and azimuth (ϕ) angles. Radar backscatter depends upon the geometrical and dielectric properties of the surface and varies with the look geometry. We use $\sigma^\circ(\theta, \phi)$ measurements, as function of θ and ϕ , to study the sand surface geomorphology. The $\sigma^\circ(\theta, \phi)$ measurements over ergs from the Ku-band NASA scatterometer (NSCAT), SeaWinds Scatterometer (QSCAT), Tropical Rain Monitoring Mission's Precipitation Radar (TRMM-PR), and C-band ERS Scatterometer (ESCAT), are used to study the surface characteristics.

A simple composite model for radar backscatter from sand dunes consisting of facets and small surface ripples is proposed. The facet model relates the surface $\sigma^\circ(\theta, \phi)$ response to the weighted sum of responses from dominant facets on the surface. Scattering from small ripples is modeled as Bragg scattering where the ripples are modeled as cosinusoidal surface waves. The amount of area covered by different facets is used to identify the type of dunes.

II. SURFACE BACKSCATTER MODEL

We extend the model presented in [2], modeling the total backscattering coefficient $\sigma^\circ(\theta, \phi)$ from the sand as sum of surface scattering $\sigma_s^\circ(\theta, \phi)$ and volume scattering. A simple volume scattering model presented in [3] is used to estimate the volume backscatter contribution. The model simulation reveals that the sand volume scattering contribution is small relative to the surface scattering so that we ignore the volume scattering and model the return backscatter as the contribution from sand surface only.

The erg surface profile has two main spatial frequency components, corresponding to the two predominant land features. The low spatial frequency (wave number) components are due to large scale dunes whereas the high wave number components are due to small ripples on the surface of the dunes. The surface scattering coefficient can be decomposed into separate surface scattering components from dunes and ripples, i.e.,

$$\sigma_s^\circ(\theta, \phi) = \sigma_d^\circ(\theta, \phi) + \sigma_r^\circ(\theta, \phi)$$

where $\sigma_d^\circ(\theta, \phi)$ is the surface scattering from large scale dunes and $\sigma_r^\circ(\theta, \phi)$ is the surface scattering from small scale ripples. Observations suggest that $\sigma_r^\circ(\theta, \phi)$ is dominated by Bragg scattering that occurs at discrete θ and ϕ . The look directions at which Bragg scattering occurs are dependent on the spectrum of the small scale ripples.

We model the sand surface as a composite of tilted rough facets with cosinusoidal ripples (corresponding to the small ripples). Figure 1 depicts one such tilted rough facet.

A. Rough Facet Model

In order to model the backscatter from large-scale erg surface features (i.e., dunes) we adopt the general scattering model presented in [4]. We modify this model to use the probability density function of the surface tilt angles. The $\sigma_d^\circ(\theta, \phi)$ component of the scatterometer measurement is the sum of the returns from all the rough facets in the footprint given by

$$\sigma_d^\circ(\theta, \phi) = \sum_n F_n \int_0^{2\pi} \int_0^{\frac{\pi}{2}} P_n(\theta_s, \phi_s) \sigma(\theta', \phi') u(\theta_g - \theta) d\theta_s d\phi_s \quad (1)$$

where summation is over all facets in the footprint and F_n is the fraction of the footprint area covered by the n^{th} rough facet. The sand dune field is modeled as a composite of tilted

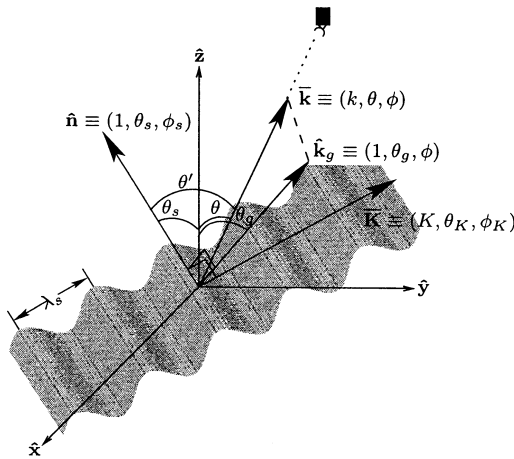


Fig. 1. Model of tilted rough facet with cosinusoidal surface ripples.

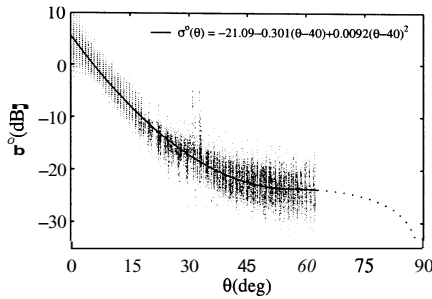


Fig. 2. σ° incidence angle response at Ku-band from combined TRMM and NSCAT data, which is assumed to be the flat surface response of sand that does not vary with ϕ . A quadratic roll off close to the grazing angles is assumed.

rough facets. $P_n(\theta_s, \phi_s)$ is the tilt distribution of the n^{th} rough facet and $\sigma(\theta', \phi')$ is the flat surface response of the sand material. θ' and ϕ' are the local incidence and azimuth angles for each facet, respectively. θ_g is the facet grazing angle and $u(\theta_g - \theta)$ is a unit step function to ensure zero response when $\theta > \theta_g$.

We use NSCAT V-pol and TRMM-PR σ° measurements to estimate the flat surface Ku-band $\sigma(\theta', \phi')$ response of the surface. NSCAT V-pol σ° observations are made over a 17°-62° incidence angle range at ten azimuth angles whereas TRMM σ° is at near nadir incidence angles 0°-17° and a very narrow azimuth angle range. Figure 2a shows $\sigma^\circ(\theta')$ for NSCAT V-pol and TRMM-PR measurements. The quadratic fit through the data is used to represent the flat surface response with no dependence on ϕ' . Lacking σ° measurements for $\theta' > 62^\circ$, a quadratic roll off is assumed at grazing angles ($\theta' > 62^\circ$).

In general, it is difficult to determine the probability distribution of the surface angles. However, by modeling sand dunes as composed of a finite number of rough facets, an estimate

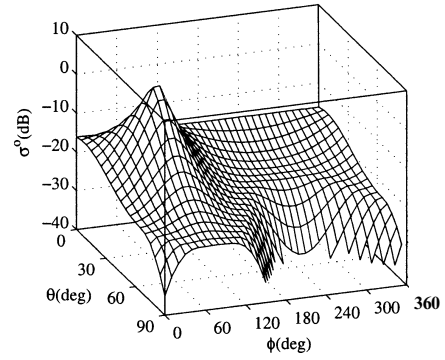


Fig. 3. Model σ° response from a single rough surface facet with $\theta_n=30^\circ$, $\phi_n=75^\circ$ and Gaussian tilt distribution having $\varsigma_\theta=\varsigma_\phi=1$ and $\varsigma_{\theta\phi}=0$.

of the probability distribution can be made. For example, a transverse dune with a slip- and a windward-side can be modeled as two rough facets tilted at (30°-35°, ϕ_n) and (10°-15°, ϕ_n+180°) mean tilt respectively. A third facet at (0°, 0°) accounts for inter-dune flat area in dune fields.

We assume the surface tilt distribution to be Gaussian with θ_n and ϕ_n mean values of θ_s and ϕ_s , and ς_θ and ς_ϕ their standard deviations, respectively. $\varsigma_{\theta\phi} = \varsigma_{\phi\theta}$ is the covariance of θ and ϕ . Figure 3a shows the modeled backscatter response from a single rough surface facet with a Gaussian tilt distribution with $\theta_n=30^\circ$, $\phi_n=75^\circ$, $\varsigma_\theta=\varsigma_\phi=1$ and $\varsigma_{\theta\phi}=0$. In the present analysis we assume θ_s and ϕ_s are uncorrelated in order to keep the simulation simple. The $\sigma^\circ(\theta, \phi)$ response peaks when $\theta=\theta_n$ and $\phi=\phi_n$ and thus clearly reflects the facet characteristics. The standard deviations of the tilt angles affect the height of the peak and gradient in its vicinity. The parabolic bite at high incidence angles in Figure 3 corresponds to the directions beyond the grazing angle of the facet and hence do not result in any backscattering.

B. Cosinusoidal Ripple Model

The shape of the small-scale ripples depends upon the angle of repose of the inherent material. The ripples are periodic in the wind direction and are skewed, resulting in two distinct sides. The downwind side is steeper than the windward side. The spectrum of sand surface ripples are narrow band. Thus, ripples are modeled as a cosinusoidal wave. The wavelength of the cosinusoid corresponds to the dominant wavelength of the ripple spectrum. The near surface wind direction changes rapidly over the undulating sand dune surface inducing local variabilities in the ripple direction. These ripples result in Bragg backscattering of incident wave which occurs only at discrete points in the θ - ϕ space. NSCAT and ESCAT σ° measurements at incidence angles higher than 15° have a high contribution from the ripples on tilted facets.

III. ROUGH FACET MODEL SIMULATION

In this section, we present model simulations over two simple dune types, transverse and longitudinal, modeled as

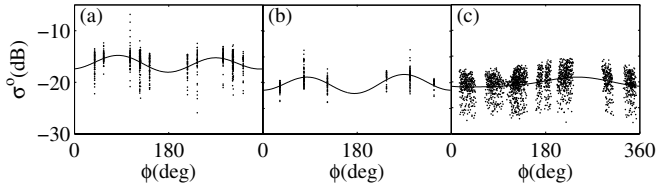


Fig. 4. σ^0 azimuth angle response over a longitudinal dune field from (a) NSCAT V-pol for θ in the range 30° - 35° , (b) ESCAT for θ in the range 30° - 35° , and (c) QSCAT for $\theta=55^\circ$. Solid line is a second order harmonic fit.

composed of rough surface facets. The results are compared to the observations made by NSCAT and ESCAT.

A. Longitudinal Dunes

A longitudinal dune has two opposite slip-sides. The slip-sides have a slope equal to the angle of repose of the parent sand which is nominally taken to be 30° - 35° and corresponds to a mean tilt angle of θ_n . The azimuth orientation of the two slip-sides are, in general, separated by 180° .

In order to correctly model the longitudinal dune field, we analyze the $\sigma^0(\theta)$ and $\sigma^0(\phi)$ responses observed by NSCAT, ESCAT and QSCAT. Figure 4 illustrates the azimuth angle modulation of σ^0 . NSCAT and ESCAT give similar results in which the two maxima correspond to the orientation of the two slip-sides of the longitudinal dune. The two maxima are separated by approximately 180° in azimuth. The NSCAT and ESCAT incidence angles in Figure 4 result in normal local incidence angle observation of the slip-sides at the azimuth angles of the graph maxima. Since these slip-sides are a result of an average wind direction parallel to the axis of the dune, the wind direction producing this dune lies between the two peaks with an ambiguity of 180° . The ESCAT σ^0 is lower than NSCAT due to its longer wavelength resulting in greater penetration. QSCAT has reduced ϕ -modulation because of its high incidence angle which does not result in normal incidence angle observation of the slip-sides.

The observation of the slip-sides in σ^0 is further confirmed by analysing the $\sigma^0(\theta)$ response at the azimuth angles corresponding to the maxima in azimuth modulation. Figure 5 presents such plots for both ESCAT and NSCAT measurements. The data is fit with a non-parametric line. A rise in the σ^0 measurements in the 30° - 35° incidence angle range is observed, particularly in Figures 5a and 5c.

We model the longitudinal dune field as two tilted rough facets and a flat rough facet between parallel dunes. Figure 6 shows the correspondence between a typical longitudinal dune and the rough facet model. The two rough facets have mean tilts $(32^\circ \pm 2^\circ, \phi_n)$ and $(32^\circ \pm 2^\circ, \phi_n + 180^\circ)$ and the third rough facet with mean tilt $(0^\circ, 0^\circ)$ (flat) is used to represent the inter-dune space in a longitudinal dune field. All of these facets are modeled with a Gaussian tilt distribution.

Figure 7a shows the cumulative tilt distribution for the modeled longitudinal dune field. We apply Equation (1) as a forward model to this tilt distribution. The σ^0 response for this

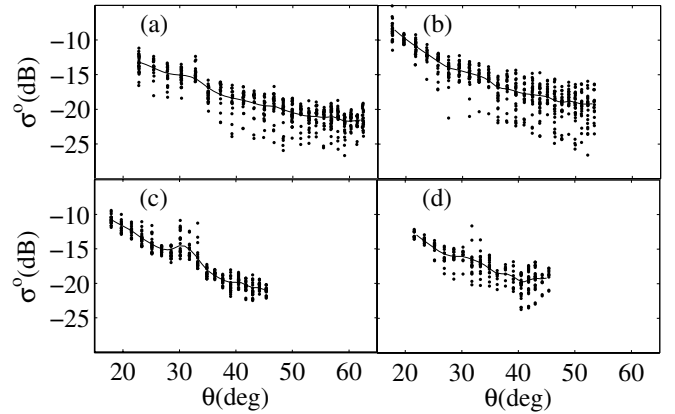


Fig. 5. σ^0 incidence angle response over a longitudinal dune field from NSCAT V-pol and ESCAT. (a) and (b) are NSCAT measurements at $\phi=56^\circ$ and $\phi=284^\circ$, respectively. (c) and (d) are ESCAT measurements at $\phi=79^\circ$ and at $\phi=218^\circ$, respectively.

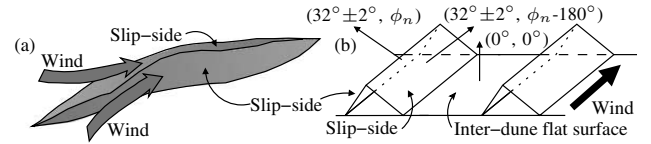


Fig. 6. (a) Longitudinal dune and (b) its facet model.

tilt distribution is shown in Figure 7b and shows the presence of three dominant facets in the form of peaks. This result is consistent to the observations made by NSCAT (Figure 7c) and ESCAT (Figure 7d) over the areas of longitudinal dune fields in the Sahara. The σ^0 vs θ lines are the non-parametric fits similar to Figure 5 but are plotted for all azimuth angles of the observations. These line fits are joined at integral incidence angle values to show the overall $\sigma^0(\theta, \phi)$ response and compare with simulated data. The peaks at $(32^\circ, 106.5^\circ)$ and $(32^\circ, 302.5^\circ)$ in NSCAT data, and at $(31^\circ, 79^\circ)$ and $(31^\circ, 281^\circ)$ in ESCAT data, are the responses due to the two slip-sides of the longitudinal dunes in the footprint. Since the slip-sides have slopes nearly equal to the angle of repose, they are almost devoid of any surface ripples.

B. Transverse Dunes

A typical transverse dune (Figure 8) has two sides, a slip-side similar to longitudinal dunes and a windward-side which is opposite to the slip-side in azimuth and has a slope of 10° - 15° . Similar to longitudinal dune, the sides of a transverse dune can be viewed as facets. We model the slip- and windward-sides of transverse dunes as rough surface facets with $(30^\circ$ - $35^\circ, \phi_n)$ and $(10^\circ$ - $15^\circ, \phi_n + 180^\circ)$ mean tilt, respectively. The dune fields are modeled as composed of many simple dunes with inter-dune areas modeled as zero tilt rough facets, similar to longitudinal dune fields. The model is shown in Figure 8.

The simulated σ^0 response for transverse dunes is shown in Figure 9a and shows the presence of two dune facets in

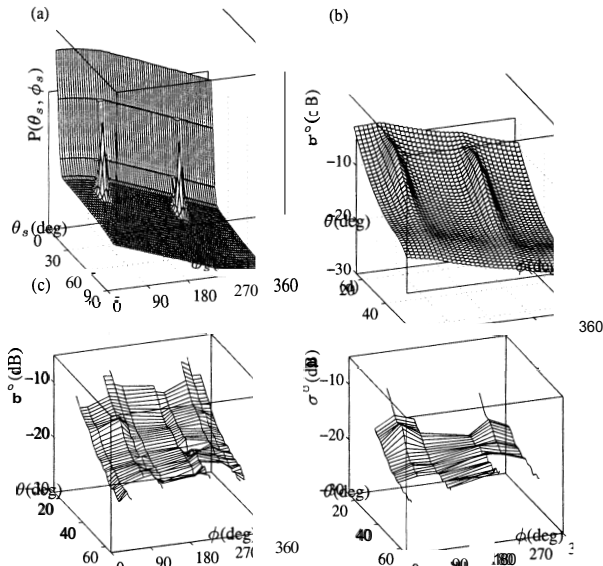


Fig. 7. (a) Tilt distribution of a longitudinal dune with each slip-side covering 25% of footprint and inter-dune flat area covering the remaining 50%. (b) is its corresponding simulated σ^0 response. Observation over actual longitudinal dune field by (c) NSCAT V-pol and (d) ESCAT.

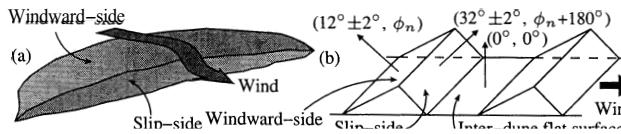


Fig. 3. (a) Transverse dune and (b) its facet model.

the form of two peaks. The flat facet peak is in the form of straight line. This result is consistent with observations made by NSCAT (Figure 9b) and ESCAT (not shown) over areas of transverse dune fields in the Sahara. The observations are similar to longitudinal dunes but have only one slip-side response. However, unlike longitudinal dunes, there is a peak 180° in azimuth from the slip-side at higher incidence angles. This peak is due to Bragg scattering from the small scale ripples on the windward-side of the transverse dune.

The model simulation results for both longitudinal and transverse dune fields significantly resemble the scatterometer observations. This is further confirmed by the consistent response from the two scatterometers operating at different frequencies.

C. Summary

The electromagnetic scattering from erg surfaces is modeled as composed of scattering from large scale dunes and small scale ripples. The dunes are modeled as composed of tilted rough facets. The total scattering due to dunes is the sum of scattering from all of the rough facets in the footprint weighted by the fraction of their area in the footprint. Small scale ripples are modeled as cosinusoidal ripples that scatter the incident electromagnetic waves in discrete directions.

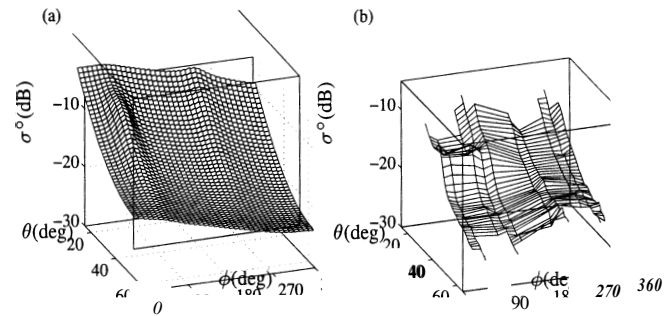


Fig. 9. (a) Simulated σ^0 response for transverse dune with slip- and windward-side covering 15% and 35% of footprint, respectively, and inter-dune flat area covering the remaining 50%. (b) Observation over transverse dune field in the Sahara by NSCAT V-pol.

Longitudinal and transverse dune fields are modeled as composed of three dominant rough facets. Two of these facets correspond to the two slip-sides in the case of longitudinal dunes. For transverse dunes they correspond to windward- and slip-side. The third facet is flat and accounts for the inter-dune flat area. The proposed rough facet model is applied to the modeled dune fields. The results indicate a strong signature of the rough facets in the backscatter response. The look directions at which the peak value occurs, give the mean tilt of the facet. The simulation results are similar to NSCAT and ESCAT observations over the Saharan longitudinal and transverse dune fields.

IV. CONCLUSION

Ergs represent diverse and dynamic parts of the Sahara that undergo a continuous surface reformation due to wind action. Ergs have two scales of surface features. The large scale features are dunes with dimensions ranging from meters to a few hundred meters. The small scale features are surface periodic ripples with wavelengths from a few to tens of centimeters.

It is found that an erg surface modulates the Ku and C-band σ^0 measurements with the look direction. The incidence angle modulation reflects the presence of slip-sides on the surface in the form of a slight rise in backscatter at the incidence angles equal to the angle of repose of sand. At these incidence angles, the azimuth modulation indicates the number of slip-sides present that can be used to identify the transverse and longitudinal dunes. This can be used to determine the average wind direction in the area.

REFERENCES

- [1] Kenneth Pye and Haim Tsoar, *Aeolian Sand and Sand Dunes*, Unwin Hyman Ltd. London, UK, 1990.
- [2] Haroon Stephen and David G. Long, "Surface Statistics of the Saharan Ergs Observed in the σ^0 Azimuth Modulation," *Proceedings of Intl. Geosc. and Rem. Sens. Symp., Toulouse, France* 21-25 July 2003, pp. 1549-1551.
- [3] Calvin T. Swift, "Seasat Scatterometer Observations of Sea ice," *IEEE Transactions on Geoscience and Remote Sensing*, vol. 37, no. 2, pp. 716-123, March 1999.
- [4] A. I. Kozlov, L. P. Ligthart, and A. I. Logvin, *Mathematical and Physical Modelling of Microwave Scattering and Polarimetric Remote Sensing*, Kluwer Academic Publishers, Dordrecht, The Netherlands, 2001.